COMPUTATION OF VORTEX SHEET ROLL-UP

Robert Krasny
University of Michigan, Mathematics Department
Ann Arbor, Michigan 48109

1. Introduction

In this article we shall review some recent developments for computing vortex sheet roll-up. A vortex sheet is an asymptotic model of a free shear layer in which the transition region between the two fluid streams is approximated by a surface across which the tangential velocity component is discontinuous. A common theme in fluid dynamics is that the vortex sheet model can be useful in understanding the dynamics of coherent vortex structures observed in laminar and turbulent flows. If this goal is to be realized, reliable methods for computing vortex sheet evolution must be developed.

At present, numerical methods are available for studying the initial value problem in two space dimensions. For example, detailed analytical phenomena such as singularity formation in the shape of an evolving periodic vortex sheet can be studied with existing methods. The complex roll-up process and the interaction of several spiral vortices has also been investigated numerically. These calculations have been stimulated by recent theoretical results about vortex sheets and by progress in the convergence theory of general vortex methods.

First, results for the periodic vortex sheet will be reviewed. Then an application to some vortex sheet problems occurring in aerodynamics will be discussed in more detail. Finally, some open questions and directions for further research will be summarized.

2. The Vortex Sheet Evolution Equation

A vortex sheet in two dimensional ideal flow can be described by a curve in the complex plane, $z(\Gamma,t) = x(\Gamma,t) + iy(\Gamma,t)$, varying with time t. The Lagrangian parameter Γ measures the circulation contained between a base point and an arbitrary point along the vortex sheet [4]. The vorticity associated with a vortex sheet is in the form of a delta function with support on the curve. The vortex sheet strength $\sigma = |\partial z/\partial\Gamma|^{-1}$ is the jump in the tangential velocity component across the curve.

The vortex sheet evolution equation is,

$$\overline{\frac{\partial z}{\partial t}} = \int K(z-\tilde{z})\, d\tilde{\Gamma}. \tag{1}$$

In this equation, $z = z(\Gamma,t)$, $\tilde{z} = z(\tilde{\Gamma},t)$, $K(z) = 1/2\pi iz$ is the Cauchy kernel and the Cauchy principal value of the integral is taken. The bar over the time derivative on the left denotes the complex conjugate. The evolution equation is supplemented by an initial condition for the vortex sheet $z(\Gamma, 0)$.

This basic evolution equation takes other forms depending upon the particular geometry and initial conditions under consideration. The simplest class of problems concerns a vortex sheet which is periodic in the x-direction. In this case, the integrand used is $K(z) = \cot(\pi z)/2i$ and the circulation parameter Γ runs over a single period $[0,1]$. The initial condition takes the form $z(\Gamma, 0) = \Gamma + p(\Gamma, 0)$. The function $p(\Gamma, t)$ is periodic in Γ and it describes the perturbation away from the equilibrium solution $z(\Gamma, t) = \Gamma$, corresponding to a flat vortex sheet of constant strength.

A straightforward method of discretization was introduced by Rosenhead [19] in 1931. Consider a finite number of point vortices per wavelength which approximately interpolate the vortex sheet at equidistant values of Γ. Thus the point vortices' positions are $z_j(t) \sim z(\Gamma_j, t)$ where $\Gamma_j = j\Delta\Gamma$ and $\Delta\Gamma = N^{-1}$. The point vortices evolve according to the following system of ordinary differential equations,

$$\overline{\frac{dz_j}{dt}} = N^{-1} \sum_{k \neq j} K(z_j - \tilde{z}_k). \tag{2}$$

By neglecting the singular term $k = j$, the sum appearing on the right side of equation (2) is formally an $O(N^{-1})$ approximation to the principal value integral in equation (1). The initial point vortex positions interpolate the exact initial vortex sheet $z_j(0) = z(\Gamma_j, 0)$. The viewpoint adopted here is that in order to study properties of the vortex sheet, one must determine whether solutions of the point vortex equations converge as the dimension $N \to \infty$. The next section reviews the theoretical results and numerical evidence relating to this issue.

3. Singularity Formation in a Periodic Vortex Sheet

The vortex sheet model does not include any physical mechanisms to stabilize the short wavelength modes. In fact, the linearized initial value problem for perturbations of a flat, constant strength vortex sheet is subject to the Kelvin-Helmholtz instability [4]. Just as in the classical example, i.e. the Cauchy problem for the Laplace equation, the linearized vortex sheet initial value problem is not well-posed in the sense of Hadamard. However, if the initial perturbation $p(\Gamma, 0)$ is an analytic function of Γ then the nonlinear vortex sheet problem has an analytic solution in some time interval [21,5]. Analyticity of the solution is equivalent to controlling the amplitude of the short wavelength modes.

These Cauchy-Kovaleski results for the periodic vortex sheet actually were preceded by an asymptotic analysis of the nonlinear problem by Moore [16]. For an initial perturbation consisting of a single Fourier mode of amplitude ϵ, Moore's analysis indicates that a singularity forms in the vortex sheet at time $t_c(\epsilon) \sim \log \epsilon^{-1}$. Meiron, Baker & Orszag [13] studied the vortex sheet's Taylor series in time around $t = 0$ and obtained a similar comclusion. At the critical time, the vortex sheet strength has a finite amplitude cusp and the curvature has an infinite jump discontinuity at isolated points. However, the sheet's slope remains bounded and its tangent vector is continuous.

Previous numerical studies of this problem using Rosenhead's point vortex approximation have experienced difficulty in converging when the number of point vortices was increased [4]. Explaining the source of this difficulty and providing a remedy for it have been longstanding issues [17,18,20].

In a numerical solution of the point vortex equations (2) one can examine the discrete Fourier transform $\widehat{p_k}$ of the computed perturbation quantities $p_j = z_j - \Gamma_j$. Using this discrete Fourier analysis to diagnose the solution, it was shown that computer roundoff error is responsible for the irregular point vortex motion that occurs at a smaller time as the number of points is increased [9]. This source of computational error can be controlled either by using higher precision arithmetic or by using a new filtering technique. The numerical evidence indicates that the point vortex approximation converges as $N \to \infty$ up to but not beyond the time of singularity formation in the vortex sheet. Good agreement is obtained with Moore's relation for the critical time's dependence upon the initial amplitude.

4. Roll-Up Past the Critical Time

When a singularity forms in the solution of a nonlinear evolution equation, it may still be possible to extend the solution beyond that time in a way which ensures that the extension has physical significance. A classical example is shock formation and the theory of weak solutions to nonlinear hyperbolic equations [12]. Even though the shock solution is a discontinuous function, it serves as a useful approximation to a viscous profile. One can ask whether a similar theory can be constructed for the vortex sheet evolution equation.

One approach to extending the vortex sheet solution past the critical time is motivated by Chorin's "vortex blob" method [6,1]. The singular kernel $K(z)$ appearing in the vortex sheet equation (1) is replaced by a smooth kernel $K_\delta(z)$ which depends upon an artificial smoothing parameter δ. For example, in free space one can choose $K_\delta(z) = K(z)\,|z|^2/(|z|^2 + \delta^2)$ as the desingularized kernel. For $\delta > 0$ the solution of this "δ-equation" is a curve which approximates the vortex sheet. The proposal is to view the vortex sheet as the limit of these desingularized solutions as the smoothing parameter δ tends to zero. To discretize the δ-equation, one simply uses the smooth kernel $K_\delta(z)$ in place of $K(z)$ in the system of ordinary differential equations (2). For $\delta > 0$ therefore the point vortex is replaced by a "vortex blob".

This approach has been applied to the periodic vortex sheet problem [10]. Linear stability analysis shows that the vortex sheet's short wavelength instability is diminished when $\delta > 0$. The resulting ordinary differential equations are numerically more tractable since the computer roundoff error difficulty is not as severe. Solutions of the δ-equation are obtained for a fixed value of δ, at a fixed time $t > t_c$ by integrating the vortex blob equations and converging to the limit $N \to \infty$. Detailed numerical convergence studies also indicate that the sequence of solutions of the δ-equation converges pointwise in Γ as $\delta \to 0$ and that the error has an asymptotic expansion in powers of δ. These results suggest that in this weak sense, as a limit of smooth curves, the vortex sheet rolls up into a double-branched spiral past the critical time.

There are other possible ways of desingularizing a periodic vortex sheet to obtain candidate weak solutions. Baker and Shelley [3] study the dynamics of a layer of constant vorticity in the limit of vanishing thickness. A key question is whether this sequence converges to the same object that solutions of the δ-equation converge to, particularly

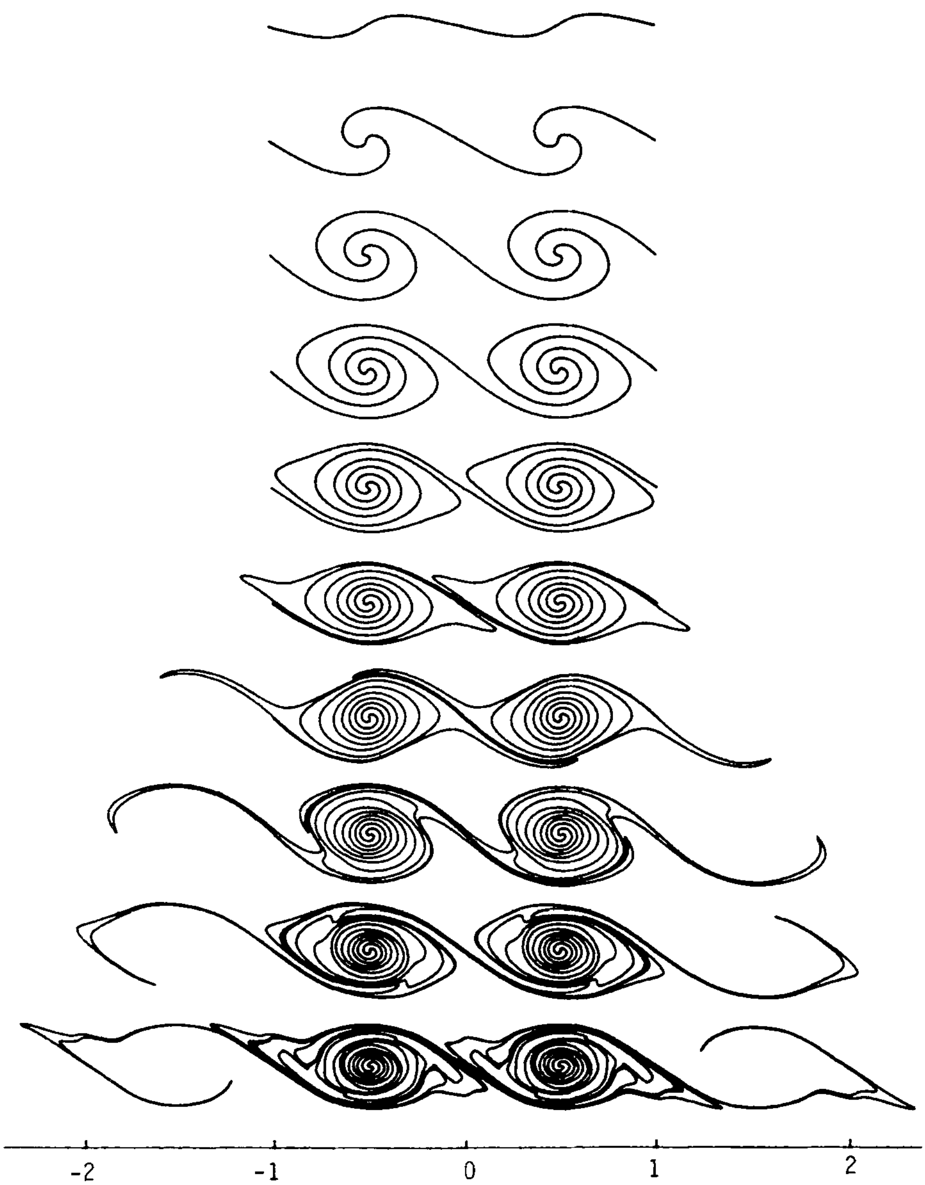

Figure 1. Periodic vortex sheet roll-up [10]. Two periods of the circulation parameter are plotted. The value of the smoothing parameter is $\delta = 0.5$.

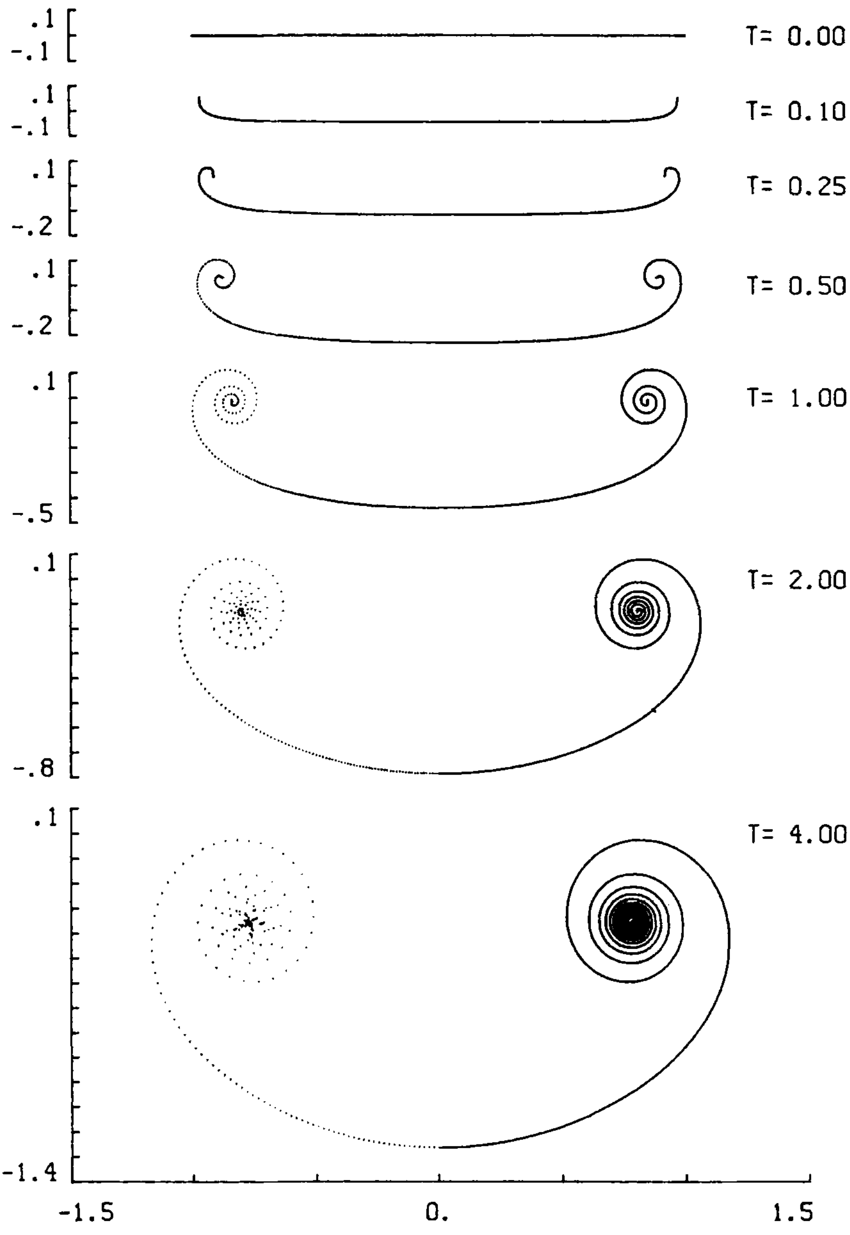

Figure 2. Roll-up of the vortex sheet shed by an elliptically loaded wing [11]. The vortex blob positions are plotted on the left and an interpolating curve is plotted on the right. The value of the smoothing parameter is $\delta = 0.05$.

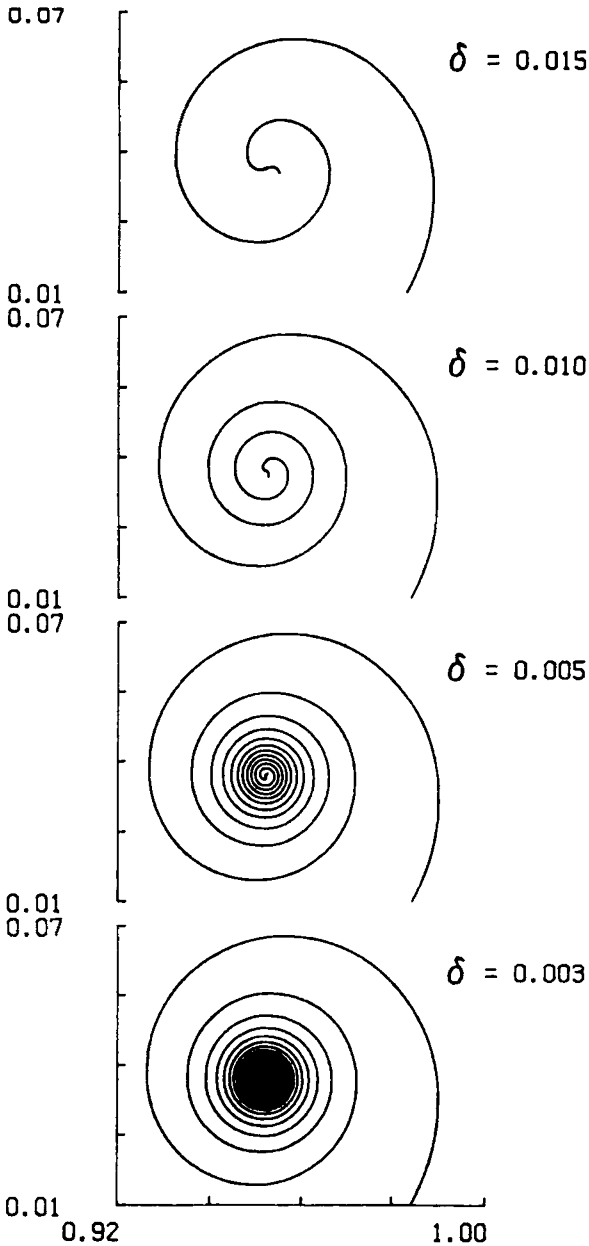

Figure 3. The effect of the smoothing parameter δ upon the tip vortex [11]. These solutions are at time $t = 0.1$. There are 23 complete turns present in the $\delta = 0.003$ case.

past the critical time. Tryggvasson [22] shows that vortex-in-cell calculations can yield solutions which resemble those of the vortex blob method. In these calculations the smoothing is provided by the interpolation procedure which passes information between the point vortices and an underlying Eulerian grid.

A long-time vortex blob calculation using the value $\delta = 0.5$ is shown in figure 1. These results were obtained using an adaptive point insertion technique and they extend a calculation in [10]. The plotted curve represents two periods in the circulation parameter and is shown from time $t = 1$ to $t = 10$ in steps of $\Delta t = 1$. The initial perturbation was an eigenfunction of the linearized equation of amplitude $\epsilon = 0.01$. With this initial condition, a singularity forms in the vortex sheet ($\delta = 0$) near time $t_c \sim 0.375$. The curve in figure 1 rolls up into a double-branched spiral whose outer turns are elliptically deformed as time progresses. At late times, the outer turns are captured by neighboring vortices and thin filaments travel into the adjacent periods. Over the times plotted, a compact core region consisting of concentric turns stays within its initial period.

5. Vortex Sheet Roll-Up in the Trefftz Plane

The desingularization approach has also been applied to the vortex sheet shed by a finite-span wing [11]. Neglecting the wake's streamwise variation leads to an initial value problem in the two-dimensional Trefftz plane, perpendicular to the line of flight. The loading on the wing's trailing edge is incorporated into the vortex sheet's initial circulation distribution. The two problems that have been studied are elliptical loading and a simulated fuselage-flap loading.

In this geometry it is advantageous to use the change of variable $\Gamma = \Gamma(\alpha)$ where $\alpha \in [0, \pi]$. Therefore, in the evolution equation (1) the element $d\Gamma$ is replaced by $\Gamma'(\alpha)d\alpha$. The vortex sheet's initial condition is $z(\alpha, 0) = \cos\alpha$, corresponding to the wing's trailing edge. The circulation distribution for elliptic loading is $\Gamma(\alpha) = \sin\alpha$. For the simulated fuselage-flap loading, the circulation distribution is a spline function, having local extrema, that has been used in previous studies [2,8].

For elliptic loading the initial vortex sheet is not an analytic function of the circulation parameter. In fact, $z(\Gamma, 0) \sim \Gamma^{1/2}$, near the wing tips $\alpha = 0$ and $\alpha = \pi$. The induced velocity on the initial vortex sheet is actually uniform across the span, i.e. $u = 0, v = -1/2$ for $x \in (0, 1)$. One possible solution is that the vortex sheet simply translates downward at speed $1/2$, preserving its flat initial shape. However, the velocity of the surrounding irrotational fluid diverges as $x \to -1^-$, $x \to 1^+$. A second solution is possible in which the vortex sheet rolls up at both tips instantaneously for $t > 0$. This nonuniqueness is only present when $\delta = 0$; for $\delta > 0$, the initial vertical velocity is not uniform and actually $v > 0$ in a small neighborhood of the sheet's tips. As will be demonstrated below, when $\delta \to 0$ the desingularized solutions converge for $t > 0$ to the rolling-up solution rather than to the translating flat vortex sheet.

Calculations for the elliptically loaded wing using the point vortex approximation do not converge for any $t > 0$ as the number of points increases [14]. We attribute this to the singularities present at the tips of the initial vortex sheet. The approach taken here is the same as was described above for the periodic vortex sheet. The δ-equation is discretized

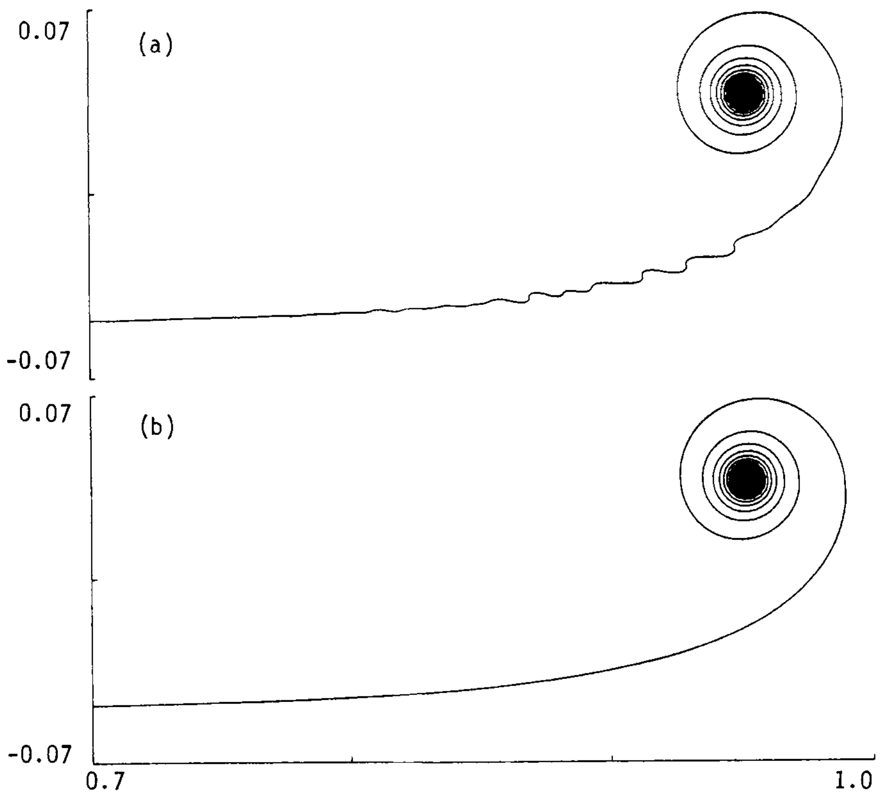

Figure 4. The effect of roundoff error when $\delta = 0.003$ [11]. a) single precision arithmetic. b) double precision arithmetic.

using vortex blobs and the resulting ordinary differential equations are integrated using the fourth order Runge-Kutta method.

A solution for the elliptically loaded wing using $\delta = 0.05$ is shown in figure 2. The left side shows the centers of the vortex blobs and the right side is an interpolating curve. The curve rolls up smoothly at both tips and propagates downward. Convergence studies documented in [11] show that the time and spatial discretization errors are negligibly small. This can be accomplished for $\delta > 0$ apparently because the solution of the δ-equation is sufficiently smooth.

For smaller values of δ the curve rolls up sooner and more turns are present. Convergence as $\delta \to 0$ has also been documented in [11]. Figure 3 shows the tip regions obtained at $t = 0.1$ for several smoothing parameter values in the interval $0.003 \leq \delta \leq 0.015$. The $\delta = 0.003$ solution in figure 3 has 23 turns present; close examination of the core region showed that the curve does not intersect itself. In fact, this particular solution is in good agreement with Kaden's asymptotic spiral (see [20]).

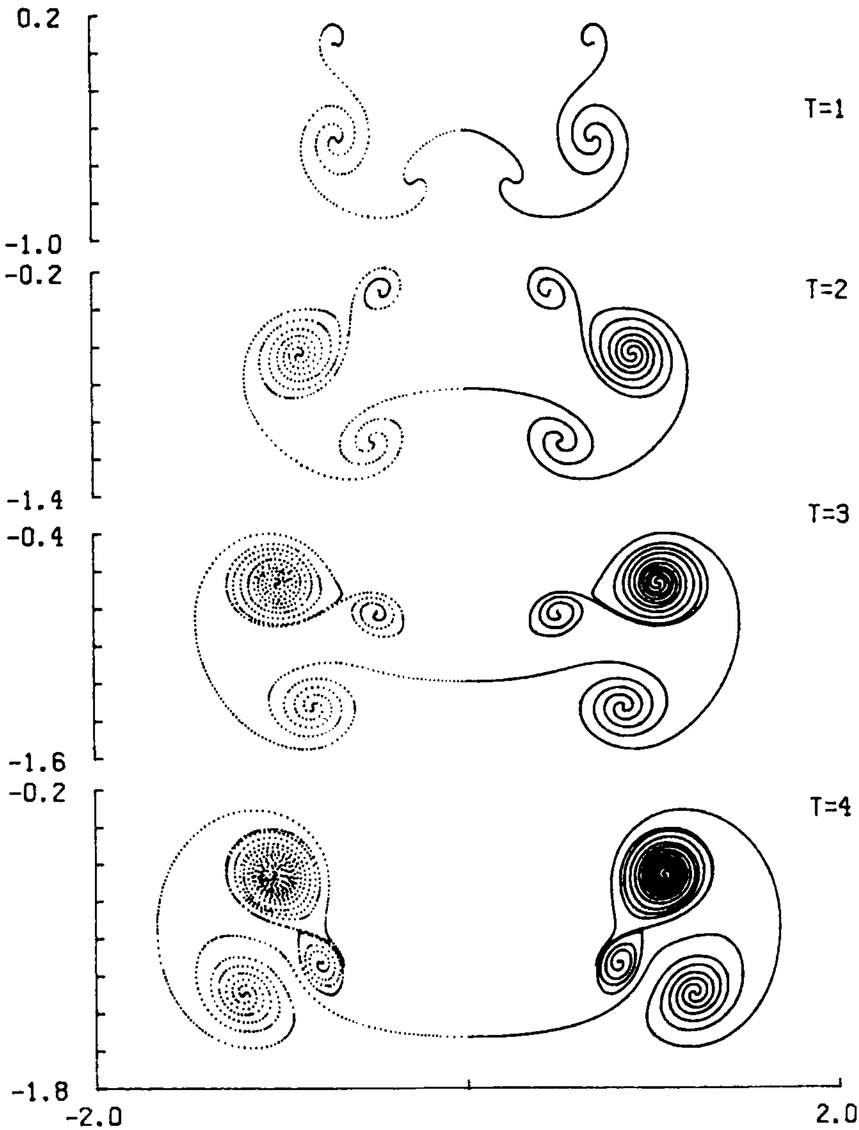

Figure 5. Roll-up of the trailing vortex sheet for a simulated fuselage-flap loading [11]. The value of the smoothing parameter is $\delta = 0.1$.

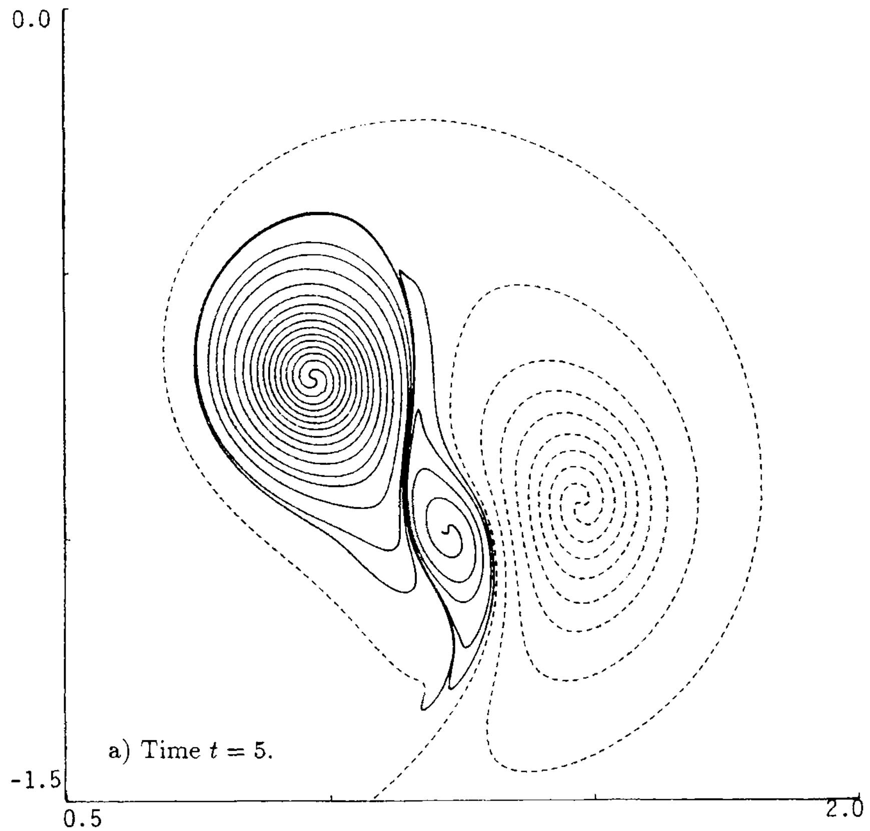

Figure 6. Closeup views of the right half-span region for the simulated fuselage-flap loading at successive times [11].

Figure 4 compares two solutions using $\delta = 0.003$ computed in single and double precision arithmetic. In the single precision calculation, small waves appear on the curve's outer turn. As in the periodic vortex sheet calculations, we attribute these waves to spurious perturbations introduced by computer roundoff error. The waves are absent from the double precision calculation since the perturbation amplitude is lower. Such calculations actually provide an empirical way of determining stability properties of the vortex sheet. For example, figure 4 indicates that the sheet's outermost turn is less stable to small amplitude, short wavelength perturbations than the rolling-up core region. This conclusion is consistent with Moore's finding [15] that sufficient stretching in the core region stabilizes the vortex sheet.

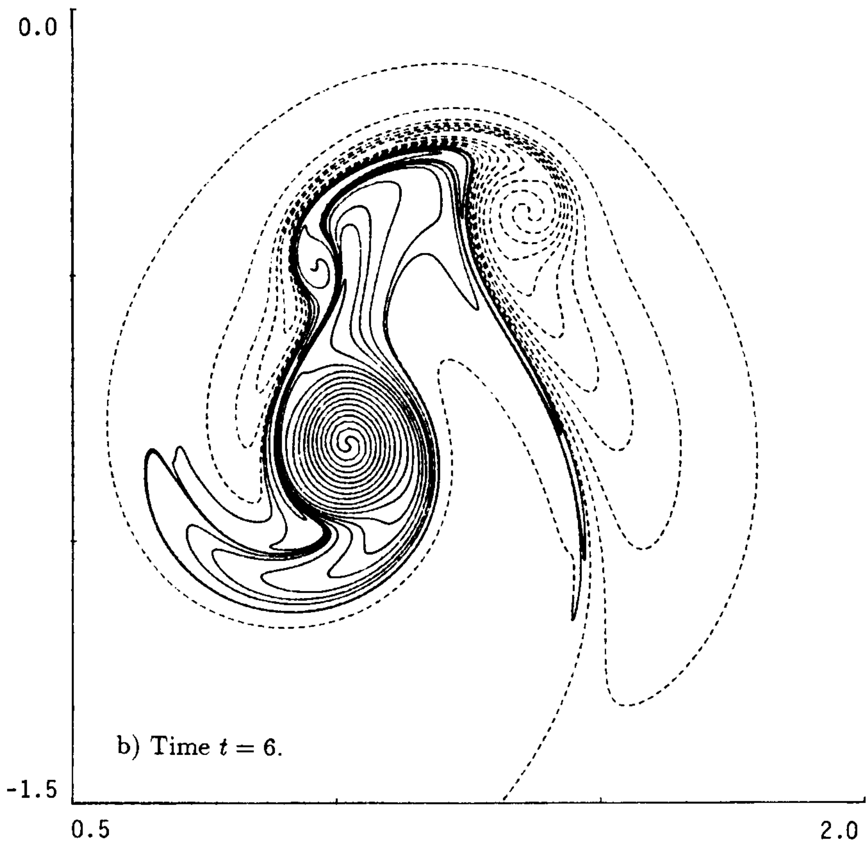

b) Time $t = 6$.

Figure 5 shows a calculation for the simulated fuselage-flap problem computed using $\delta = 0.1$. In these calculations an adaptive point insertion technique was used to maintain accuracy without incurring unacceptable expense in run time. The computation in figure 5 took two hours to run in single precision arithmetic on a VAX 8600 computer.

Several vortices form in each half-span region due to the local extrema present in the initial spanwise circulation distribution. There is a single-branched tip vortex and two double-branched vortices further inboard. The flap vortex is the strongest in each half-span region and it has the same sense of rotation as the tip vortex. These two like-signed vortices tend to rotate around each other. The fuselage vortex has the opposite sense of rotation, which causes the entire half-span structure to propagate outward like a vortex dipole. At time $t = 4$ portions of the curve are very highly stretched. The outer turns of the tip and flap vortices have been captured by the neighboring vortex in a way that is similar to the periodic vortex sheet (figure 1).

As the calculation proceeds past $t = 4$ the curve becomes quite complicated due to a sequence of vortex interactions. Closeup views of the curve in the right half-span region are shown in figures 6a-d. In these figures, the solid (resp. dotted) portion of the curve denotes positive (resp. negative) vortex sheet strength.

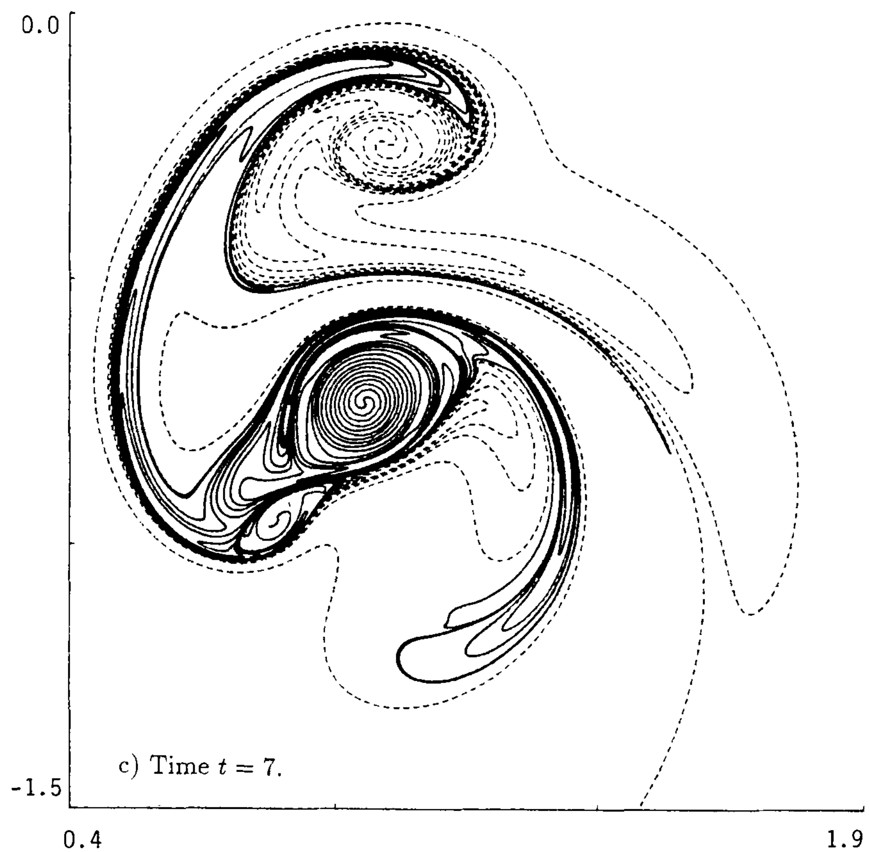

c) Time $t = 7$.

At time $t = 5$ (figure 6a) the tip vortex has entered the jet region between the two larger oppositely rotating vortices. The outer turns of all three vortices are quite distorted. Between times $t = 5$ and $t = 6$, as the tip vortex is swept around the strong co-rotating flap vortex, it will collide with the fuselage vortex and carry away a portion of this vortex. The outcome is shown in figure 6b. A dotted portion of the curve is separated from the fuselage vortex core by the tip vortex. It should be emphasized that the curve is a material line and it does not break or intersect itself. This is so even under close examination of various regions in which parts of the curve move very close together. It can be seen in figure 6b that the curve develops regions of high curvature, possibly even cusps.

Further snapshots at times $t = 7$ and $t = 8$ are given in figures 6c,d. Three core regions are still discernible, although the outer turns have been stripped away and can no longer be associated with a particular core. Long one-dimensional fronts are formed which consist of many closely spaced distinct portions of the curve. Notice how the fuselage vortex has traveled around the flap vortex in this sequence of pictures. At time $t = 8$ (figure 6d) the positions of these two strong vortices are such as to produce propagation inward, in contrast to the previous outward propagation which occurred up to time $t = 4$ (figure 5).

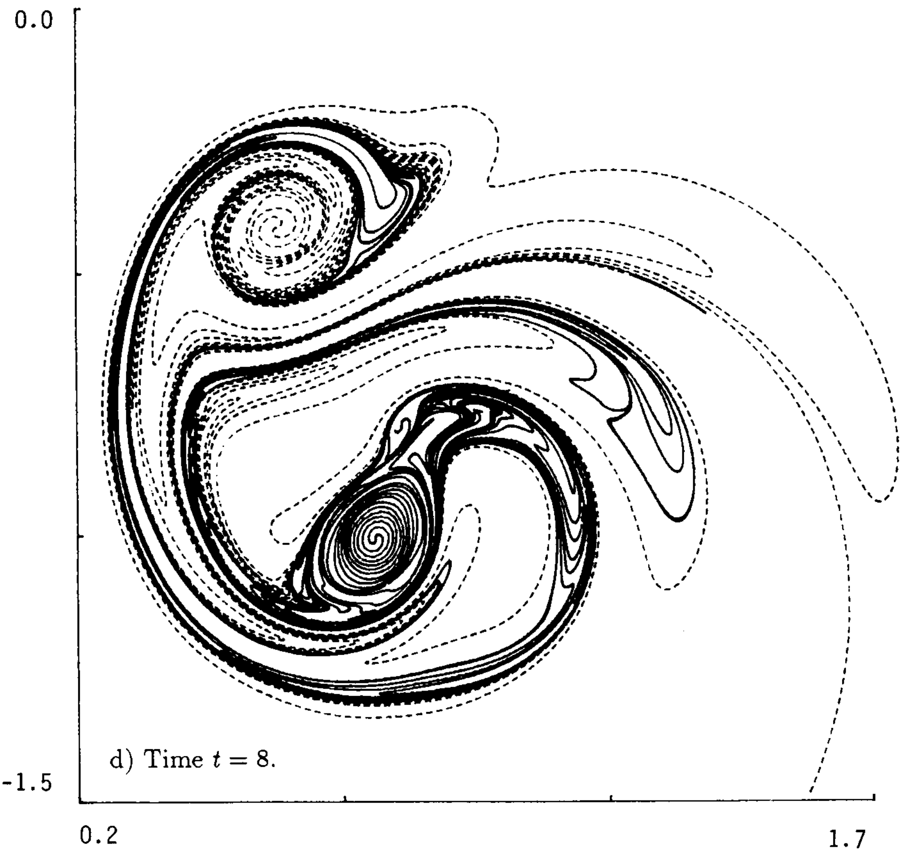

d) Time $t = 8$.

It should be emphasized that the results presented are accurate solutions of the δ-equation for the particular values of δ chosen. Many questions arise. What features of the $\delta > 0$ results are preserved in the limit $\delta \to 0$? Does any region of the curve become fractal? Do new types of singularities form perhaps as suggested by DiPerna and Majda in their theory [7] of measure-valued solutions of the Euler equations? What would change if viscosity, boundaries or three-dimensionality were incorporated into the model? These are some of the possible directions for further research.

The work reviewed here was begun at the University of California, Berkeley when the author was a Ph.D student under Professor Alexandre J. Chorin. The author was later supported by an NSF Postdoctoral Research Fellowship taken at the Courant Institute, New York University. The computations were performed at the Courant Institute and at the University of Minnesota Supercomputer Center under grant DMS 8414101 from the NSF Office of Advanced Scientific Computing. The author also gratefully acknowledges partial support while at Courant from the NASA-Ames Research Center (NAG 2-345) and the Air Force Office of Scientific Research (URI 86-0352).

References

[1] Anderson, C. R. 1985 A vortex method for flows with slight density variations. *J. Comp. Phys.* **61**, 417.

[2] Baker, G. R. 1979 The "Cloud in Cell" technique applied to the roll-up of vortex sheets. *J. Comp. Phys.* **31**, 76.

[3] Baker, G. R. & Shelley, M. 1987 these preceedings.

[4] Birkhoff, G. 1962 Helmholtz and Taylor instability. *Proc. Symp. Appl. Math. XIII A.M.S.*, 55.

[5] Caflisch, R. & Orellana, O. 1986 Long time existence for a slightly perturbed vortex sheet. *Comm. Pure Appl. Math.* **39**, no. 6, 807.

[6] Chorin, A. J. & Bernard, P. S. 1973 Discretization of a vortex sheet, with an example of roll-up. *J. Comp. Phys.* **13**, 423.

[7] DiPerna, R. J. & Majda, A. 1987 Concentrations in regularizations for 2-D incompressible flow. *Comm. Pure Appl. Math.* **40**, no. 3, 301.

[8] Hoeijmakers, H. W. M. & Vaatstra, W. 1983 A higher-order panel method applied to vortex sheet roll-up. *AIAA J.* **21**, 516.

[9] Krasny, R. 1986 A study of singularity formation in a vortex sheet by the point vortex approximation. *J. Fluid Mech.* **167**, 65.

[10] Krasny, R. 1986 Desingularization of periodic vortex sheet roll-up. *J. Comp. Phys.* **65**, 292.

[11] Krasny, R. 1987 Computation of vortex sheet roll-up in the Trefftz plane. *J. Fluid Mech.* **184**, 123.

[12] Lax, P. D. 1973 Hyperbolic systems of conservation laws and the mathematical theory of shock waves. *Reg. Conf. Ser. Appl. Math. SIAM 11.*

[13] Meiron, D. I., Baker, G. R. & Orszag, S. A. 1982 Analytic structure of vortex sheet dynamics. I. Kelvin-Helmholtz instability. *J. Fluid Mech.* **114**, 283.

[14] Moore, D. W. 1974 A numerical study of the roll-up of a finite vortex sheet. *J. Fluid Mech.* **63**, 225.

[15] Moore, D. W. 1976 The stability of an evolving two-dimensional vortex sheet. *Matematika* **23**, 35.

[16] Moore, D. W. 1979 The spontaneous appearance of a singularity in the shape of an evolving vortex sheet. *Proc. R. Soc. Lond. A* **365**, 105.

[17] Moore, D. W. 1981 On the point vortex method. *SIAM J. Sci. Stat. Comput.* **2**, 65.

[18] Pullin, D. I. 1982 Numerical studies of surface-tension effects in nonlinear Kelvin-Helmholtz instability and Rayleigh-Taylor instability. *J. Fluid Mech.* **119**, 507.

[19] Rosenhead, L. 1931 The formation of vortices from a surface of discontinuity. *Proc. R. Soc. Lond.* A **134**, 170.

[20] Saffman, P. G. & Baker, G. R. 1979 Vortex interactions. *Ann. Rev. Fluid Mech.* **11**, 95.

[21] Sulem, C., Sulem, P. L., Bardos, C. & Frisch, U. 1981 Finite time analyticity for the two and three dimensional Kelvin-Helmholtz instability. *Comm. Math. Phys.* **80**, 485.

[22] Tryggvasson, G. 1987 Simulation of vortex sheet roll-up by vortex methods. *J. Comp. Phys.* to appear.